



Published in final edited form as:

J Mol Biol. 2008 September 19; 381(5): 1168–1183. doi:10.1016/j.jmb.2008.06.037.

Cholesterol Effects on Bax Pore Activation

Eric Christenson, Sean Merlin, Mitsu Saito, and Paul Schlesinger

Department of Cell Biology and Physiology, Washington University School of Medicine

Abstract

The importance of BCL-2-family proteins in the control of cell death has been clearly established. One of the key members of this family, BAX, has soluble, membrane bound and membrane integrated forms that are central to the regulation of apoptosis. Using purified monomeric human BAX, defined liposomes and isolated human mitochondria we have characterized the soluble to membrane transition and pore formation by this protein. For the purified protein, activation but not oligomerization, is required for membrane binding. The transition to the membrane environment includes a binding step that is reversible and distinct from the membrane integration step. Oligomerization and pore activation occur after the membrane integration. In cells, BAX targets several intracellular membranes, but notably does not target the plasma membrane while initiating apoptosis. When cholesterol was added to either the liposome bilayer or mitochondrial membranes we observed increased binding but markedly reduced integration of BAX into both membranes. This cholesterol inhibition of membrane integration accounts for the reduction of BAX pore activation in liposomes and mitochondrial membranes. Our results indicate that the presence of cholesterol in membranes inhibits the pore forming activity of BAX by reducing the ability of BAX to transition from a membrane associated to a membrane integral protein.

Introduction

Genetically programmed apoptotic cell death occurs in all multicellular organisms [1]. Control of the death decision prominently involves a three part regulatory ensemble of proteins, the BCL-2-family [2]. Twenty-five genes comprise this family and they generate three functional classes of proteins: pro-apoptotic and anti-apoptotic actors with a supporting cast of BH3-only proteins that modulate their interaction [3,4]. To function as the apoptotic decision agent these proteins collaborate to form a gateway, “pore”, in the outer mitochondrial membrane (OMM) [5,6,7]. The formation of this pore requires the availability of active and uninhibited BAK or BAX in the outer mitochondrial membrane [8]. BAX and many of the other proteins are soluble and move to the mitochondrial outer membrane in concert with the death signaling [9,10]. Others have demonstrated the formation of BAX homo-oligomers in mitochondria and inferred a correlation with a mortality decision in the OMM [11,12,13,14]. However, the nature of the BCL-2-family protein interactions while in membranes is not clear. Furthermore the molecular events and environmental conditions that trigger BAX transformation to an active state have remained elusive. Recent studies have indicated that suppression of BAX inhibition is critical in the mortality decision

Corresponding Author: Paul H Schlesinger, MD, PhD, Department of Cell Biology and Physiology, Washington University School of Medicine, 660 S. Euclid Avenue, St. Louis, MO 63110, E-Mail: PAUL@CELLBIO.WUSTL.EDU Tel (314) 362-2223, Fax (314) 362-7463.

Publisher's Disclaimer: This is a PDF file of an unedited manuscript that has been accepted for publication. As a service to our customers we are providing this early version of the manuscript. The manuscript will undergo copyediting, typesetting, and review of the resulting proof before it is published in its final citable form. Please note that during the production process errors may be discovered which could affect the content, and all legal disclaimers that apply to the journal pertain.

[15,16,17]. While it is possible that negative regulation is a dominant theme in apoptosis this gives no explanation of the mechanism by which BAX becomes situated in the outer mitochondrial membranes and is availed of the negative regulation. Furthermore if the regulation is entirely negative by anti-apoptotic $BCL-2$ -family members in the OMM then the escape of the remaining and vastly larger membrane surface of the cell from BAX predation is a mystery.

Both pore forming and regulatory interactions of $BCL-2$ -family proteins occur at the mitochondrial outer membrane. Previously we have shown that one pro-apoptotic protein, genetically engineered active BAX ($BAX(\Delta C19)$), can form large pores in planar lipid bilayers [18]. Subsequently we characterized these pores in defined liposomes as consisting of dimers and tetramers of $BAX(\Delta C19)$. The tetrameric pore was able to accommodate cytochrome *c* for release from the liposome [19]. From the kinetics of pore activation upon addition of soluble monomeric $BAX(\Delta C19)$ we concluded that the oligomerization into pores occurred after membrane insertion and postulated that it would be dependent upon the membrane environment. Therefore we have undertaken studies to explore the role of membrane lipids on $BCL-2$ -family protein pore activation.

In these studies we have determined the $BAX(\Delta C19)$ pore activation in the presence of cholesterol and the enantiomer of cholesterol [20]. Cholesterol is necessary for membrane function in eukaryotic cells but the chemical and physical basis for the cholesterol requirement remains unclear [21]. Cholesterol is synthesized in the endoplasmic reticulum and is internalized with the plasma membrane and by receptor-mediated endocytosis. From both the endoplasmic reticulum and the late endosomal pathway cholesterol enters other compartments of the cell [22]. In steroidogenic tissues, *eg.* adrenal and placenta, hormone production is initiated by side chain cleavage in the mitochondrial matrix [23,24]. In other cells mitochondrial cholesterol oxidation occurs at lower rates but can become pathogenic when the cells are cholesterol overloaded [25]. When cholesterol is taken up by mitochondria it first resides in the outer mitochondrial membrane and is then transferred through the contact sites using the peripheral benzodiazepine receptor to the matrix for oxidation [26,27]. It has been suggested that movement of cholesterol from the OMM to IMM, where oxidation occurs, is facilitated by a cholesterol recognition/interaction amino acid consensus (CRAC) motif that is observed in the peripheral benzodiazepine receptor [28]. In mammalian cells the plasma membrane has the highest cholesterol content but significant cholesterol, oxysterols and bile acids are found in the mitochondria because of the matrix oxidative production of these steroids [29,30]. Cholesterol has been reported to be elevated in cultured tumor cells [31,32]. Recently bilayer cholesterol content has been shown to influence BAX oligomerization and trypsin resistance in liposomes and mitochondria [33]. Others have reported complex relationships among lipids, cholesterol, BAX and permeability transition pore activation [34]. These observations have been used to explain the effects of cholesterol upon cellular apoptosis. We have studied the effect of cholesterol on BAX pore formation in liposomes and mitochondria and conclude that the cholesterol content of the plasma membrane protects it from the pore formation when BAX is activated. In particular the addition of cholesterol to the outer membrane of mitochondria inhibits pore formation by BAX . We discuss the mechanism of cholesterol inhibition of BAX pore activation in terms of membrane binding and integration and speculate on how this might influence apoptosis in mammalian cells.¹

¹**Abbreviations:** TMPD, N,N,N',N'-tetramethyl-p-phenylenediamine; *nat*cholesterol-natural enantiomer of cholesterol; *ent*cholesterol-the full enantiomer of cholesterol; DOPC, dioleoylphosphatidylcholine; DOPA, dioleoylphosphatidic acid; OMM, Outer Mitochondrial Membrane; IMM, Inner Mitochondrial Membrane; CF, Carboxyfluorescein.

Results

Although the BCL-2-family proteins are clearly the arbiters of a mortality decision; the biochemical steps which conclude in the mitochondrial death decision are not yet clear. We have pursued a reconstitution methodology to study these phenomena in order to clearly define the biochemical and biophysical processes in the reaction steps leading to the initiation of apoptosis. Initially these studies revealed that a genetically engineered form of active BAX_{BAX} ($\Delta C19$), could form a cytochrome c competent pore in liposomes [19]. Hill analysis revealed that in liposomes active $BAX_{BAX}(\Delta C19)$ inserted into the membrane as a monomer, formed a functioning pore as a dimer and displayed a concentration dependent progression to a tetramer complex that transferred cytochrome c out of the liposomes. We are revisiting this method of analysis in order to study the effects of lipid environment on BAX membrane integration and pore formation.

Human BAX Expression, Purification and Studies of Pore Activation

Native BAX in mammalian cells is a soluble protein that must be activated to induce apoptosis [3,35]. This protein can be activated *in vitro* in several ways. In this study we have used a genetically engineered form of active human $BAX_{BAX}(\Delta C19)$, which has a portion of the α -helix 9 removed. In 0.1% n-octylglucoside this form of human $BAX_{BAX}(\Delta C19)$ is monomeric with a molecular weight of $19,000 \pm 1200$ as determined by dynamic light scattering and by SDS PAGE, Figure 1A. In these studies we used the human $BAX_{BAX}(\Delta C19)$ because we would employ human mitochondria to study pore formation in these organelles. The pore activation and stoichiometry of human $BAX_{BAX}(\Delta C19)$ have not previously been reported. The human and mouse BAX proteins are very similar in sequence but arginine-64 in the critical BH3 region is replaced with a lysine. In addition there is a rearrangement of the prolines adjacent to the first α -helix (residues 46–53). Proteolytic cleavage and phosphorylation in this region of BAX influences the mitochondrial translocation and pore formation [36,37]. We concluded that confirmation of a similar mechanism of pore formation by the human protein was warranted. Using liposomes loaded with carboxyfluorescein (CF) at quenching concentrations we studied the activation of pores by human $BAX_{BAX}(\Delta C19)$, Figure 1B. The time series data normalized to the total dequenching for each preparation of liposomes is an exponential release. This is consistent with a single pore producing full dequenching from a liposome and the exponential time course representing pore activation in the liposomes. The measured time constants were used in a Hill analysis of the human $BAX_{BAX}(\Delta C19)$ pore activation, Figure 1C. The concentration dependence of human $BAX_{BAX}(\Delta C19)$ activation in liposomes indicates a pore activation stoichiometry of 2 and 4, similar to the previously published model for the murine protein[19].

A Mitochondrial Preparation for the Study of OMM Permeability

The permeability of the outer mitochondrial membrane is a key factor in the apoptosis death decision [38]. These studies have used HeLa cell mitochondria and human BAX protein. We have adapted the fusion of liposomes with purified mitochondria to create a preparation for the study of OMM permeability [39,40]. The unfused liposomes were removed by low speed pelleting of the resulting mitochondria. The fused mitochondria (fM) have a normal double-membrane morphology, Figure 2A. The captured CF produced photo-conversion of diaminobenzidine and electron dense deposition in the intermembrane space, Figure 2A_{photo-converted}. Carboxyfluorescein containing mitochondria and liposomes were identified by this method but the insoluble photo-conversion product obscures the membranes [41,42].

Cytochrome c dependent oxygen consumption can be used to evaluate the continuity of the OMM [43]. When our preparation was studied using a Clark electrode to determine site IV dependent oxygen consumption in the presence of saturating substrate and oxygen they consumed 43.1 ± 0.4 nAtom $\text{mg}^{-1}\text{min}^{-1}$ which is similar to rat liver mitochondria (48.5 ± 0.4

nAtom $\text{mg}^{-1}\text{min}^{-1}$) but less than skeletal muscle or kidney mitochondria [44]. This rate of oxygen uptake suggests that in the preparation the OMM is intact and cytochrome c is retained within the intermembrane space. Using the membrane active peptide melittin we interrupted the uptake of oxygen by the mitochondria as shown in Figure 2B. This reduction is reversed by the addition of 100 μM horse cytochrome c to the electrode chamber. The oxygen consumption in these preparations is dependent upon ADP, phosphate and is sensitive to azide. We conclude that our isolated mitochondria have an intact OMM and that cytochrome c is retained during the isolation procedure.

Ca²⁺-dependence of fM permeability—The fM preparation was performed in media containing EGTA so that Ca²⁺ concentration is less than 10 nM. At this low calcium the CF is retained within the OMM barrier. Increasing the media calcium to 100 or 200 μM initiated rapid dequenching of the CF from the intermembrane space, Figure 2C. Dequenching is normalized to the maximum dequenching produced by 1 % Triton X-100. The dequenching is rapid and dependent upon calcium concentration and is consistent with activation of the voltage-dependent anion-selective (VDAC) channel of the OMM [45].

Presence of porin-like channel activity in the mitochondrial preparation—The release of anionic CF by Ca²⁺ elevation suggests that VDAC is present but in a low conductance state in our fM preparation [45]. We have directly assessed the channel activity of the fM in planar lipid bilayers. Using our preparation of mitochondria that was post-liposome fusion we allowed these to interact with a planar lipid bilayer. After addition of the fM to the cis bilayer chamber fusion transients were observed within 5 minutes of continuous stirring. After fusions had occurred the resulting bilayer currents were studied using a ± 60 mV voltage ramp or by voltage steps under voltage clamp, Figure 3A & B. The ramp current pattern was typical of many studies of VDAC currents in mitochondrial membrane preparations or reconstituted VDAC protein [46,47]. The conductance of these currents was decreased when the Ca²⁺ was reduced with EGTA, consistent with the reported calcium dependent shift of VDAC to a low conductance channel [45,48], Figure 3C. The fM currents also displayed voltage dependent inactivation as described for the VDAC channels [49].

BAX(ΔC19) Pore Activation in the Outer Mitochondrial Membrane

Isolated mitochondria used in these studies were loaded with carboxyfluorescein by pH-dependent fusion of liposomes with the OMM as described in Methods. This fusion mediated transfer effectively loads the mitochondria inter-membrane space with carboxyfluorescein, but at reduced concentration from that present in the liposomes. Therefore the dequenching response of the mitochondria per mole of lipid is less than that of the primary liposomes. Consequently, in the assay of BAX pore activation using the fM we have increased the concentration of mitochondria lipid to 4.3 μM , which compensated for the reduced dequenching from the fM preparation. The application of BAX(ΔC19) to this mitochondrial preparation produces a rapid time course of carboxyfluorescein dequenching. As shown in Figure 4A the kinetics and concentration dependence of BAX(ΔC19)-initiated dequenching from mitochondria is qualitatively consistent with that observed in defined liposomes. There is a distinct difference between specific activity of BAX(ΔC19) pore formation in mitochondria and liposomes. The higher activity of BAX in liposomes can be compensated by correcting for the difference in lipid content in the assay, Figure 4B. After this adjustment of the rate of pore activation for the increased lipid in the mitochondrial assay the Hill analysis for pore formation in mitochondria closely resembles what we have observed in liposomes, Figure 4C. Because of the additional lipid in the mitochondrial assay the lowest BAX(ΔC19) concentrations (≈ 1 nM) do not generate sufficient activity for accurate analysis.

Effect of Cholesterol on BAX Pore Activation in Defined Liposomes

BAX is found in the cytosol of most eukaryotic cells but when activated in response to pro-apoptotic stimuli it becomes integrated into the mitochondrial outer membrane and the endoplasmic reticulum [50]. Because the membranes in which BAX integrates *in vivo* have less cholesterol than the plasma membrane, we have studied the effect of this sterol on interaction of BAX with membranes.

Cholesterol containing liposomes were prepared and characterized as described in the Methods. The final cholesterol concentration in the liposomes was 20 mol% and the size of the liposomes was verified by dynamic light scattering. The effect of the cholesterol was to dramatically decrease the $BAX(\Delta C19)$ pore activation, Figures 5A & B. As a consequence the τ (time constants) were large as was the error in their determination. From this data we could analyze the Hill plot but not the pore size. Here we have succeeded in extending the Hill analysis to low enough BAX concentrations that we can discern the curvature in spite of the greater error in the measurements of the time constant. When we plot the time constants the effect of cholesterol is dramatic and increases at lower BAX concentrations, Figure 5C.

The sterol mediated inhibition of $BAX(\Delta C19)$ pore formation could be due to a direct and stereospecific interaction between steroids and the BAX protein. To test this we prepared liposomes using the enantiomer of cholesterol. This analog of cholesterol has the configuration inverted at each asymmetric site in the cholesterol molecule [20]. This compound was the generous gift of Dr. D. Covey of the Department of Developmental Biology, Washington University School of Medicine. The comparison of pore activation in liposomes containing *nat*-cholesterol or *ent*-cholesterol indicates that the enantiomer is as effective as the natural compound at the inhibition of BAX pore activation, Figure 5D. This suggested that the effect resulted primarily from cholesterol's condensing and other effects upon the lipid membrane environment and not a stereo-specific interaction with BAX [51,52,53].

Effect of Cholesterol on BAX Pore Activation in Mitochondria

The inhibition of $BAX(\Delta C19)$ pore activation by the inclusion of cholesterol in the liposome membrane composition is dramatic. The simple composition of our liposomes might contribute to this inhibition and generate an artificially large inhibition that will not be seen in a more complicated membrane. We wanted to test the effect of cholesterol in a physiologic membrane in which we could alter the composition in a known fashion. Our fM mitochondria fulfilled these requirements. The native mitochondria supported $BAX(\Delta C19)$ pore formation well and by fusing them with DOPC/DOPA/C liposomes we could increase the cholesterol content of the OMM to at least 16 mol% during the fusion step. It has previously been shown that the cholesterol of the OMM is slowly metabolized in isolated mitochondria indicating that the elevated cholesterol was maintained during our experiments [23]. The addition of cholesterol to OMM produced a substantial inhibition of the pore activation, Figure 6. However, this reduced the $BAX(\Delta C19)$ activity to such an extent that it was not possible for us to characterize the effects on oligomerization and pore size.

BAX Interaction with Liposome Membranes

BAX pore formation requires the translocation of the soluble BAX protein to a bilayer membrane. This step is critical *in vivo* and is thought to be a consequence of BAX activation in cells [36, 54,55]. The mechanism of the membrane translocation of BAX must progress along a binding followed by integration model [56]. The progress of translocation will be influenced by contributions from both the protein structure and the membrane environment. The interaction of BAX with membranes can be clearly shown in a defined liposome experimental system, Figure 5E. Furthermore, the effect of cholesterol appears to be a reduction of membrane incorporated BAX protein. We have extended the use of defined liposomes to the study of BAX membrane

translocation by employing surface plasmon resonance. In this approach defined liposomes were supported at the sensor surface using the hydrophobic chips (L1) from the Biacore Corporation[57]. Using these immobilized liposomes it was possible to study the interaction of $BAX(\Delta C19)$ with the liposome bilayer membrane in concentration and time dependent experiments.

For three preparations of activated $BAX(\Delta C19)$ the concentration dependence and time course of binding and membrane integration were determined and averaged, Figure 7A. The membrane associated BAX populations were characterized as total binding to supported liposome membranes at the end of the injection period (60 seconds) and the mean stable bound protein after an extended wash period (300—350 seconds). These populations were determined and are plotted in Figure 7B as the average of the individual trials along with the fitted lines. The total BAX membrane binding at 60 seconds was tested against one and two-state interaction models. A Chi-squared analysis indicated a two-state model to be preferable with residuals reduced 10-fold. The resulting high and low affinity estimates for membrane binding are listed in Table 1. The concentration dependence of BAX integration into the liposome membrane was clearly dominated by a single interaction and the results of that analysis are also presented in Table 1. From this analysis of the binding and integration curves the size of the membrane populations of BAX were estimated and are presented as mole fractions to correct for small changes in liposome immobilization on the Biacore chip. Inspection of these fitted results for membrane association reveals three populations of membrane associated BAX . High and low affinity populations that rapidly dissociate, and the membrane integrated fraction which is slowly dissociating. The ratio of total membrane bound to integrated BAX increases at low BAX concentrations and then begins to fall as membrane capacity becomes saturated Figure 7C.

Bax Interaction with Liposome Membranes Containing Cholesterol

In cells, BAX pores are described in the OMM but pores in other membranes have not been noted. Specifically, pores in the plasma membrane produce osmotic lysis and necrosis [58,59]. The osmotic lysis of cells would be inconsistent with the apoptotic program of cells and the molecular basis for this membrane selectivity is important to explaining the physiology of cell death. One of the distinctions between intracellular membranes and the plasma membrane is the high cholesterol composition of the plasma membrane in most cells. Using cholesterol-containing liposomes and mitochondria we and others observed reduced BAX pore activation [33]. In the preceding section we have shown that $BAX(\Delta C19)$ interaction with membranes involves a rapid but reversible binding to the membrane followed by integration into the membrane, resulting in a very slow dissociation of the integrated protein population from the bilayer. Using surface plasmon resonance the effect of cholesterol on the liposome binding and integration of BAX was investigated.

The cholesterol containing liposomes loaded onto the L1 chip similarly to the DOPC:DOPA liposomes and blocked albumin access to the chip surface (see Methods). The interaction of human $BAX(\Delta C19)$ with liposome membranes containing cholesterol is shown in Figure 8. As with the DOPC:DOPA liposomes detergent activation of human $BAX(\Delta C19)$ was required for significant interaction with the cholesterol containing membranes. For three preparations of activated $BAX(\Delta C19)$ the concentration dependence of binding and membrane integration were determined and averaged, Figure 8A. Visual inspection of $BAX(\Delta C19)$ interaction with DOPC:DOPA:C liposomes indicated that it was distinct from the $BAX(\Delta C19)$ interaction with DOPC:DOPA liposomes. The initial membrane association was still rapid and larger for the cholesterol containing membranes. Paradoxically from this larger pool of membrane associated BAX the membrane integration was reduced, Figure 8B. Analysis of the concentration dependent membrane association once again demonstrated both low and high affinity binding populations as shown in Table 1. The binding pools were approximately 60% larger than in the

DOPC:DOPA liposomes. In spite of this, the integrated fraction was significantly reduced and reached a maximum value that was 58% of that seen in the liposomes without cholesterol. In addition, the ratio of membrane integrated to membrane associated BAX demonstrated a very distinct concentration dependence in that there was no increase of the integrated fraction at low concentrations of added BAX , Figure 8C.

Discussion

Because $BCL-2$ -family proteins are central arbiters of the mitochondrial mortality decision [3], we have undertaken a detailed analysis of their biochemical activities. Although twenty-five genes comprise this family and they generate both pro- and anti-apoptotic proteins [8], apoptosis regulation centers on the activation of a “pore” in the mitochondrial outer membrane by BAX and BAK [60]. We have taken the view that by studying this pore activation in detail it will become possible to clarify the influences of the regulatory $BCL-2$ - family members. Therefore, we have compared BAX pore activation in liposomes with that activity in mitochondria. Our reconstitution approach permitted a detailed study of the stages of BAX membrane translocation using surface plasmon resonance. This analysis was applied to the mechanism of cholesterol inhibition of BAX pore activation.

A Mitochondrial Preparation for the Study of $BAX(\Delta C19)$ Pore Activation

The *in vivo* death decision polling occurs in the outer mitochondrial membrane (OMM) which has a complex composition of protein and lipid. We have developed a mitochondrial preparation in which to study the translocation and pore forming activity of BAX protein. Photo-conversion of the carboxyfluorescein produced deposition of an electron dense polymeric product in the intermembrane space representing the localization of the carboxyfluorescein between the inner and outer mitochondrial membrane [61]. We conclude that the fM preparation is an intact double membrane mitochondrion having an OMM that provides a diffusion barrier similar to that described for native mitochondria [62,39,63].

$BAX(\Delta C19)$ Pore Activation in the Outer Mitochondrial Membrane

Our mitochondrial preparation, fM, satisfied morphologic, metabolic and OMM functional criteria to be a useful preparation for the study of BAX pore forming activity. By using the fM preparation we are able to study the activation of human $BAX(\Delta C19)$ in some detail. The pore activation rate and kinetics in mitochondrial and liposome $BAX(\Delta C19)$ activity are comparable as shown in Figure 4C. The activation of this pore is proposed to be a critical decision point in cell death with the OMM forming the environment for the $BCL-2$ -family proteins to negotiate this decision [3, 64, 8]. Using fM a strong correlation with the pores that we have characterized in defined liposomes is apparent. The specific activity of the purified pore forming protein is very similar once the necessary correction of the lipid concentration in our assays is considered. Our Hill analysis suggests that the added BAX undergoes a two stage oligomerization in the membrane that is consistent with our studies in defined liposomes. This comparison suggests that the BAX forms a dimer and tetramer pore in the OMM, a model that is consistent with chemical cross-linking of BAX in the OMM [65, 12].

Effect of Cholesterol on BAX Pore Activation in Defined Liposomes and Mitochondria

Cholesterol is an important component of eukaryotic membranes, having many effects upon membrane characteristics and the activity of membrane components. In beginning these studies we were attracted by the possibility that the difference in cholesterol content between the plasma membrane and the OMM was an important factor in directing the formation of BAX ($\Delta C19$) pores. Our data and the data of others support this conclusion [33]. Adding cholesterol (≈ 20 mol%) to liposomes and the OMM significantly inhibits $BAX(\Delta C19)$ pore formation. This is more cholesterol than the concentrations reported to be present in the OMM and less than

the cholesterol content of the plasma membranes [31,23,66,67]. Therefore, we conclude that the sterol concentrations of defined liposome membranes can play a role in regulating the pore formation by *BAX*. To verify that cholesterol was effective in a complex lipid environment we used liposomes to adjust the cholesterol content of the mitochondrial outer membrane. Direct analysis of the cholesterol content of the fM indicate that the incorporation was successful and produced a cholesterol concentration of ≈ 20 mol%. Although cholesterol side chain oxidation can be brisk in isolated mitochondria, this occurs in the inner membrane, whereas outer membrane cholesterol is quite stable and not oxidized in the isolated organelle [23]. Therefore, our experiments show that the incorporation of exogenous cholesterol into the OMM reduced *BAX*($\Delta C19$) pore formation substantially compared with mitochondria fused with liposomes containing only phospholipids. This observation that the cholesterol effect was similar in the simple liposome and the complex mitochondrial membrane environment seems to favor a direct interaction between the sterol and the *BAX* protein. Direct interactions are also suggested by the putative cholesterol recognition/interaction motif in α -helix 5 (at positions 113–120) [68,28]. However, in both liposomes and mitochondria the *ent*-cholesterol was as effective as the natural compound in reducing *BAX* pore formation, strongly indicating that cholesterol exerts its effect by influencing the lipid environment and having secondary effects upon *BAX* pore formation [20,69]. In addition, the reduced pore activation by *ent*-cholesterol at high *BAX* concentrations in both liposomes and mitochondria may reflect chiral sterol–phospholipid interactions that are reported for the *ent*-cholesterol in phospholipid mono-layers [70].

We conclude that cholesterol could have a significant effect on the mortality decision in cells that are overloaded with this steroid. Mitochondrial cholesterol overload has rarely been studied but has been observed in tumor cell lines [32,71,72] and in cultured cells where mitochondrial cholesterol has been increased pharmacologically [33]. Likewise, cholesterol depletion is reported to enhance apoptosis in statin treatment [73]. However, the mitochondrial membrane environment is complex and steroid oxidation an active process in these organelles [23,24]. Therefore, when multiple membrane parameters are changed decreased permeability transition pore activation has also been reported [34]. Our studies have focused on cholesterol in a controlled experimental situation to understand the mechanism by which cholesterol inhibits *BAX* pore activation.

The Interaction of *BAX*($\Delta C19$) with Liposomes Studied by Surface Plasmon Resonance

In order to address the mechanism of cholesterol inhibition of *BAX* pore activation we have used surface plasmon resonance to compare the interaction of *BAX*($\Delta C19$) with immobilized liposomes (\pm cholesterol). Surface plasmon resonance has been applied to the study of membrane binding and integration of a number of pore forming proteins and peptides [74,75,76,77,78]. We have used the attached liposome configuration to quantitatively study the rapid binding of soluble *BAX*($\Delta C19$) and concentration dependent membrane integration of the membrane-bound protein. The data in Figure 7 clearly demonstrate that the membrane binding of *BAX*($\Delta C19$) is completely dependent upon detergent activation of the purified protein. The maximum response to non-activated *BAX*($\Delta C19$) was ≈ 5 RU which is consistent with the predicted response from the mass of non-associated protein ($3.3 \mu\text{M}$ *BAX*($\Delta C19$)) injected over the supported liposomes. Therefore, essentially no membrane association occurs by the non-activated *BAX* protein. In cells *BAX* also does not associate with the mitochondrial membrane until it is activated [54,60].

These surface plasmon resonance studies confirm that the interaction of activated *BAX* with liposome membranes clearly displays the two observed stages of binding and integration [54]. The binding stage is rapid and displays high and low affinity components. Membrane integration of *BAX* is slower but dissociates very slowly, if at all. Analysis of the concentration dependence of binding indicates a high and a low affinity population of membrane associated

BAX . The concentration dependence of BAX membrane integration suggests a single population. We plotted the ratio of integrated to total membrane associated BAX to study the relationship between these two. In the DOPC/DOPA liposomes the ratio has an increasing phase, suggesting that binding of BAX to the liposomes enhances the integration step. Membrane binding and integration of BAX saturates even though no protein or typical molecular receptor is present in the membrane. This saturation occurs as the maximum mole-fraction (solubility) of the BAX protein associated with the membrane surface or integrated into the membrane is reached. This saturation produces the falling ratio of integrated to total membrane associated BAX as higher concentrations of added BAX engage nonproductive modes of membrane association. Interestingly in the DOPC/DOPA/C membranes the increasing ratio at low BAX concentration is eliminated. However, since both binding populations are increased in the DOPC/DOPA/C membranes the integration promoting step and its cholesterol inhibition must occur after the binding steps that we have observed.

Analysis of the Cholesterol Inhibition of $BAX(\Delta C19)$ Pore Activation

The results of our analysis of BAX association with membranes are presented in Table 1. In this Table the effect of cholesterol on BAX integration into bilayer membranes is apparent. BAX binds to a greater extent (both high and low affinity pools are increased by 60%) to membranes that contain cholesterol but membrane integration is dramatically inhibited (42% reduction). These changes produce the inhibition of BAX pore formation that we observe in liposomes and mitochondria. The effect upon BAX pore activation is consistent with our proposed mechanism of pore activation that includes the in-membrane dimer and tetramer oligomerization of BAX protein. In this model of in-membrane oligomerization a reduction of membrane integration by cholesterol will suppress pore activation. Cholesterol is known to have a condensing effect upon membranes by reducing the phospholipid area that is especially prominent for the liquid disordered phase that we have in our DOPC/DOPA liposomes [79,52]. This condensation can be observed as a lateral phase-separation in membranes of appropriate composition [80]. Membrane condensation itself could reduce BAX integration without a direct cholesterol- BAX interaction. The equivalence of cholesterol and *ent*-cholesterol inhibition at low BAX integration levels favors membrane condensation over direct sterol-protein interaction. The increased inhibition by *ent*-cholesterol as BAX integration approaches membrane saturating levels might reflect stereo-specific cholesterol interactions with BAX or with membrane phospholipids [70]. If we extrapolate the effect of cholesterol upon the concentration dependence of membrane integration it appears to explain the inhibition of pore activation. Thus, we have no evidence to suggest stereo-specific interaction with the BAX and inhibition of the in-membrane oligomerization steps. However, this does not necessarily contrast with the prior report on effects of cholesterol on BAX [33]. That work compared the BAX integrated to the total membrane associated protein using trypsin sensitivity. This measure is very similar to the ratio that we calculate and although we observe that the ratio in DOPC/DOPA/C membranes has a distinct BAX concentration dependence there is a range where it is similar to that in DOPC/DOPA membranes. Our data only support a cholesterol effect on the membrane integration of BAX that is mediated by altering the membrane environment.

There have now been two investigations showing that the pore forming activity of BAX is inhibited by cholesterol in liposome membranes. Both of these have increased the cholesterol of the OMM to produce BAX inhibition in that membrane also. By comparison with our results the cholesterol levels of cell surface membranes will certainly reduce BAX pore formation. It remains to be demonstrated how the cholesterol levels of intracellular membranes change and influence cell death. Resistance of tumor cells to therapy, the persistence and growth of atheromatous lesions and their final rupture, the extent of re-perfusion cell death in infarct and stroke regions and skeletal muscle apoptosis may all be affected by cholesterol levels and the inhibition of BAX activity.

Summary

The 25 *BCL-2*-family proteins are central regulators of apoptosis. As one of these, *BAX* is a critical instigator of apoptosis by transitioning from a soluble protein to a membrane integrated pore. We have characterized this transition in liposomes and human mitochondria. Activation of the soluble protein is required for membrane binding, membrane integration and in-membrane oligomerization to form pores. Cholesterol is a major inhibitor of *BAX* pore activation in mitochondria and liposomes. This inhibition does not require direct interaction with the *BAX* protein but appears to function on the membrane environment to inhibit *BAX* integration into the membrane bilayer.

Materials and Methods

Preparation of *BAX*(Δ C19)

Two methods for producing recombinant *BAX*(Δ C19) were employed. For dequenching experiments, the cDNA for human *BAX*, with the putative transmembrane carboxy-terminal α -helix truncated, was sub-cloned into pGEX-KG vector, expressed in BL21(DE3) *E. coli*, and purified as a GST fusion protein. After harvesting by centrifugation, cells were resuspended in lysis buffer (PBS, pH 7.4, 1% Triton X-100, 1 mM DTT, Complete Protease Inhibitor Cocktail (Roche; Indianapolis, IN), sonicated, and the clarified lysate applied to GSH-agarose. Resin was subjected to high salt wash (including 0.1% Triton X-100), flushed with cleavage buffer (50 mM Tris, pH 7.5, 150 mM NaCl, 0.1% n-octyl- β -D-glucopyranoside [OG], 2.5 mM CaCl₂, 1 mM DTT), and *BAX*(Δ C19) cleaved from GST tag using thrombin (Novagen, Madison WI).

For surface plasmon resonance experiments, human *BAX*(Δ C19) cDNA was sub-cloned into pTYB1 vector (NEB; Ipswich, MA), expressed in BL21(DE3) *E. coli*, and purified as an intein/chitin-binding domain fusion protein. After harvesting by centrifugation, cells were resuspended in lysis buffer (PBS, pH 7.4, Complete Protease Inhibitor Cocktail [Roche; Indianapolis, IN]), sonicated, and clarified lysate applied to a chitin affinity column. Resin was subjected to high salt wash followed by flushing with cleavage buffer (20 mM Tris, pH 8.0, 500 mM NaCl, 1 mM EDTA, 50 mM DTT) and incubated at 4°C for 48 hours to allow intein self-cleavage and release of recombinant *BAX*(Δ C19). Eluted proteins were estimated to be >95% pure by Coomassie staining SDS-PAGE gels and stored at 4°C. *BAX*(Δ C19) was activated by addition of 2% OG for 1 hr. at 4°C then dialyzed overnight against EB (10 mM HEPES, pH 7.0, 100 mM KCl, 0.01% NaN₃). *BAX*(Δ C19) retained pore forming capacity for >72 hrs after dialysis with no diminution of activity.

Liposome preparation by Reverse Phase Method

Liposomes were prepared using the reverse phase procedure of [81]. Lipids were obtained as solutions in chloroform from Avanti Polar Lipids, Inc. (Alabaster, Alabama). Mixtures of 1,2-dioleoyl-sn-glycero-3-phosphocholine (DOPC) and 1,2-dioleoyl-sn-glycero-3-phosphate [Monosodium salt] (DOPA) and 5-cholestene-3 β -ol (cholesterol, Sigma-Aldrich, St. Louis, MO.) were prepared at a mole fraction ratio of DOPC:DOPA 0.74:0.26 or DOPC:DOPA:C 0.59:0.21:0.20 in chloroform. Chloroform was first evaporated under a stream of N₂ gas and then further remove by vacuum (10⁻⁵ Torr) for 2 hours. Dried lipids were stored in N₂ gas at -20°C. Carboxy-fluorescein (MW=376) (Molecular Probes, Eugene, Oregon) was prepared at 20 mM in EB, adjusted to pH=7.2 and stored at 4°C. Dried lipids were reconstituted by addition of 1 ml ethyl ether and 0.5 ml CF solution. The suspension was sonicated at 1200 W for 20 seconds producing a stable suspension and ether was evaporated on a rotary evaporator at 40 rpm under reduced pressure (water aspiration) for 13 min at room temperature. The 0.5 ml suspension was supplemented with an additional 0.5 ml of the 20 mM carboxyfluorescein

solution. This mixture was passed through a 22 gauge needle affixed to a mini-extruder (Avanti, Alabaster, Alabama) containing a 200 nm membrane (Nuclepore, Pleasanton, California) for 3 complete cycles. The extra-vesicular carboxyfluorescein was removed by passing the liposome-dye mixture over a 1×20 cm Sephadex G-25–80 (Sigma, St. Louis, Missouri) column in EB. A liposome peak was collected and analyzed by dynamic light scattering (N5 Submicron Particle Size Analyzer, Beckman-Coulter, Fullerton, California), diameter = 207±12.5 nm. Phospholipid concentration in this fraction was determined to be 3.3 mg/ml [82].

Dequenching Analysis of _{BAX} Pore Activation

We have used the analysis of dequenching to study the activation of pores in bilayer membranes [83,84,85,19]. Using mono-disperse unilamellar vesicles the activation of membrane pores was studied by measurement of the increased fluorescence as carboxyfluorescein exits from the membrane compartment and is diluted into the assay volume. All assays were done at a total lipid concentration of 0.4±0.05 μM. The time dependence of the dequenching from our liposome and mitochondria preparations is well described by equation (1), without additional exponential terms.

$$F_{520} = F_0 A_1 (1 - e^{-(\text{time}/\tau)}) + m \times \text{time} \quad (1)$$

The formation of a 10 to 30 Å pore in a 200 nm vesicle (or mitochondrion, see Figure 2) will permit the equilibration of carboxyfluorescein with the media within 30–100 milliseconds [86,87]. In the time scale of our assay a single pore opening will not be resolved and the exponential dequenching we observe represents the kinetics of pore activation. A linear component in the time series was frequently not observed but represents pores that are unstable and which close before single vesicle dequenching is complete with subsequent pore activation being required to complete dequenching [88]. For a time series experiment the fractional dequenching at each time point was determined by normalizing the fluorescence (F_I) with the Triton X-100 generated total dequenching for each assay, equation (2).

$$F_{520} = \frac{F_{I_{\text{time}}} - F_{I_{\text{baseline}}}}{F_{I_{\text{TritonX-100}}} - F_{I_{\text{baseline}}}} \quad (2)$$

The analysis of _{BAX} pore activation was undertaken by determining the time constant, τ, and the total exponential fluorescence change, A₁, for each time series dequenching. The kinetic constants were determined by nonlinear least squares analysis using the Levenberg–Marquardt algorithm which yielded χ² values of < 0.001 for each time series.

Assessment of BAX(ΔC19)-liposome Interaction by Centrifugation and Silver Staining

OG-activated BAX(ΔC19) was dialyzed overnight against EB. BAX was applied to liposomes ± cholesterol (1.1 μM total lipid concentration), incubated for 10 min. at room temperature, and ultracentrifuged at 150000 × g for 20 minutes at 4°C. The supernatant was collected and proteoliposome pellet subjected to alkaline extraction by resuspension in 100 mM sodium carbonate for 30 min on ice. Samples were again ultracentrifuged and supernatant and pellet fractions collected. After SDS-PAGE and silver staining, relative intensities of BAX bands were quantified using QuantityOne software (Biorad; Hercules, CA).

Preparation of Mitochondria

Mitochondria were prepared from cultured cells following published procedures [89,90]. The mitochondria were isolated from HeLa cells maintained in culture where the unstimulated rate of apoptosis is < 5%. We used 250 mM sucrose for osmotic stabilization (pH=7.0, 10 mM HEPES) and added 1 mM EGTA to maintain low Ca²⁺. All procedures were performed at 4 °C on ice baths except as noted. Cell cultures were washed with ice cold sucrose solution to remove media and serum and the cells mechanically scraped from the dishes. After

homogenization (40 strokes with a loose Dounce) the nuclei and undisrupted cells were removed by centrifugation at 500×g. Mitochondria were then collected by centrifugation at 9000×g. The mitochondrial pellet was resuspended and protein concentration determined using the Micro BCA protein assay kit (Pierce Chemical Co., Rockford, Illinois, USA). The mitochondria were suspended at 1 mg/ml protein in the unilamellar liposome preparation for fusion as described previously [39,40]. The carboxyfluorescein (CF) loaded liposomes were 1 mM in lipid and contained 2×10^{12} liposomes per ml. The mitochondria and liposomes were incubated together at 15 °C for 60 minutes and then the pH dropped to 6.5 by addition of 60 µL of 100 mM PIPES (pH=6) for 5 minutes. The fused mitochondria were pelleted at 9000×g and washed two further times in 250 mM sucrose buffer to remove un-fused liposomes. Lipid analysis by Dr. Richard Gross of the Department of Medicine at Washington University allowed us to adjust the fusion protocol in order to incorporate the desired amount of cholesterol into the mitochondria. This analysis showed that the liposome fusion increased DOPA to 3 times the DOPA in the isolated mitochondria before fusion[91]. We used this ratio to calculate that when we were using liposomes containing 20 mol% cholesterol the OMM cholesterol was increased to 16 ± 0.4 mol%. Cholesterol in liposome and mitochondria preparations were converted to trimethylsilyl ethers and determined using GC-Mass spectrometry by Dr. Dan Ory of the Department of Medicine Washington University School of Medicine [92]. Mitochondria fused to these levels were used in all of the experiments to test the effect of cholesterol on *BAX* activity in mitochondria.

Electron Microscopy and Photo—conversion of the Mitochondrial Preparations

Mitochondria were purified as above and fixed with 2.5% glutaraldehyde in 0.1M sodium cacodylate for 30 minutes on ice after which they were spun at top speed in a table top microfuge to form a tight pellet. After rinsing, the pellet was sequentially stained with osmium tetroxide and uranyl acetate; then dehydrated and embedded in Polybed 812. Tissue was thin sectioned on a Reichert-Jung Ultracut, viewed on a Zeiss 902 Electron Microscope, and recorded with Kodak E.M. film. For photo—conversion the mitochondria were washed after fixation and treated with 6 mM potassium cyanide and then suspended in cacodylate buffer with 2.8 mM 3,3'-diaminobenzidine tetra-hydrochloride for exposure to a 75 watt xenon lamp. After 6 minutes the mitochondria are washed by centrifugation and processed for electron microscopy as above.

Measurement of mitochondrial oxygen consumption

Mitochondria were prepared as described above. Mitochondria at a protein concentration of ≈ 1 mg/ml were placed into the Instech Dissolved Oxygen Measuring system (Warner Instruments, Hamden, CT 06514) in 150 mM KCl (pH=7.0), 1 mM EGTA and 5 mM DTT at 20°C. The Buffer was equilibrated with 95% O₂ and stored in an airtight syringe prior to use. The concentration of dissolved O₂ was corrected for atmospheric pressure. During the assay the mitochondria were sequentially treated with 5 mM malate, 5 mM ADP, 2 µM rotenone, 5 mM succinate, 10 mM ascorbate and tetramethyl p-phenylene diamine (TMPD) and a baseline obtained in 10 mM azide. After the addition of ascorbate–TMPD the rate of oxygen consumption was dependent upon site IV which employs cytochrome c and cytochrome oxidase in the transfer of electrons to molecular oxygen[93]. The rates of oxygen consumption were normalized for protein concentration.

Planar lipid bilayer studies on isolated fused mitochondria

Planar lipid bilayers were prepared from the phospholipids DOPC:DOPA (74:26 mol%). Phospholipids were obtained from Avanti Polar lipids in chloroform solution and were mixed to the correct ratio and the chloroform removed under nitrogen. The lipids were then stored under nitrogen at –20°C until dissolved in decane at 20 mg per ml. Briefly, 2 µl of lipid solution

was applied to 0.25-mm orifice of a polystyrene cuvette (Warner Instruments, Hamden, CT), and the solvent was allowed to evaporate. The cuvette was then placed into a bilayer chamber and connected to a bilayer clamp (BC525-c; Warner Instruments) by Ag/AgCl electrodes via agar bridges. Data were collected using CLAMPEX 9.0 (Axon Instruments, Foster City, CA), archived on videotape using a Neurocorder DR-484 (Neuro Data Instruments, Delaware Water Gap, PA), and analyzed using ORIGIN (OriginLab Corporation, Northampton, MA) and CLAMPFIT (Axon Instruments). Bilayers were formed by spreading with a polished glass rod and allowed to thin to a capacitance of $0.4 \mu\text{F}/\text{cm}^2$, at which point the noise was typically 0.2 pA and the leak conductance was 2 pS. The salt concentrations are described in the appropriate figure legends. Outward (positive) currents were defined as K^+ moving cis to trans. All solutions were buffered to pH 7.0 with 10 mM K-HEPES. Mitochondria (10 μg of protein) were added to the cis chamber with mixing. To vary calcium concentration, EGTA and CaCl_2 were added as indicated. The MilliQ water employed for buffers in these studies averaged 30 μM Ca^{2+} and mitochondrial isolation buffer contained 1 mM EGTA to reduce free Ca^{2+} to $< 1 \mu\text{M}$. Calcium was varied by adding 100 μM CaCl_2 or 100 μM EGTA to the bilayer chamber.

Surface Plasmon Resonance Studies of BAX -Liposome Interaction

These studies were done using Biacore \times instrumentation and software (Biacore Division of GE Healthcare, Uppsala, Sweden) at an ambient temperature of 20°C . Buffers were filtered through 0.22 μm filter prior to use. Liposomes were prepared as described above. The buffer was EB unless noted. The sensor surface of an L1 chip (Biacore) was equilibrated in EB. Liposomes were injected at a phospholipid concentration of 0.6 mg/ml across the sensor surface at a flow rate of 3 $\mu\text{l}/\text{min}$ for 12 minutes. Loosely associated liposomes were washed from the surface by increasing the flow rate of running buffer to 500 $\mu\text{l}/\text{min}$ for 30 sec. To ascertain the extent of liposome coverage of the surface and to block remaining non-specific binding sites 1mg/ml BSA was injected at 15 $\mu\text{l}/\text{min}$ for 2 min[94]. The DOPC:DOPA liposomes loaded to 13 ± 0.9 ng of lipid per μm^2 and the DOPC:DOPA:C liposomes loaded to 12.3 ± 1.2 ng of lipid per μm^2 . Variation in loading was primarily due to variation in the liposome size distribution. $\text{BAX}(\Delta\text{C19})$ protein was injected over supported liposomes at 30 $\mu\text{l}/\text{min}$, and the dissociation observed for 5 min at the same flow rate at which the protein was injected. The response was corrected for injection artifacts. Data were analyzed and displayed using BIAevaluation (Biacore) and Origin 7.5 (OriginLab Corp., Northampton, MA) software. At each concentration of BAX protein the line presented results from the averaging of 2 to 4 independent binding studies. The standard deviation from this averaging is shown in the binding plots when its value is larger than the symbols or line which is being displayed.

References

1. Steller H. Mechanisms and genes of cellular suicide. *Science* 1995;267:1445–1449. [PubMed: 7878463]
2. Adams JM, Cory S. Bcl-2-regulated apoptosis: mechanism and therapeutic potential. *Curr Opin Immunol* 2007 Jul;19:1–9. [PubMed: 17157490]
3. Danial NN, Korsmeyer SJ. Cell death: Critical control points. *Cell* 2004;116:205–219. [PubMed: 14744432]
4. Korsmeyer SJ, Wei MC, Saito M, Weiler S, Oh KJ, Schlesinger PH. Pro-apoptotic cascade activates BID, which oligomerizes BAK or BAX into pores that result in the release of cytochrome c. *Cell Death Differ* 2000;7:1166–1173. [PubMed: 11175253]
5. Dejean LM, Martinez-Caballero S, Kinnally KW. Is mac the knife that cuts cytochrome c from mitochondria during apoptosis? *Cell Death Diff* 2006;13:1–9.
6. Green DR, Kroemer G. The pathophysiology of mitochondrial cell death. *Science* 2004;305:626–629. [PubMed: 15286356]

7. Jiang X, Wang X. Cytochrome c-mediated apoptosis. *Annu. Rev. Biochem* 2004;73:87–106. [PubMed: 15189137]
8. Reed JC. Proapoptotic multidomain Bcl-2/Bax-family proteins: mechanisms, physiological roles, and therapeutic opportunities. *Cell Death Diff* 2006;13:1378–1386.
9. Youle RJ. Cell biology. cellular demolition and the rules of engagement. *Science* 2007;315:776–777. [PubMed: 17289967]
10. Leber B, Lin J, Andrews DW. Embedded together: The life and death consequences of interaction of the Bcl-2 family with membranes. *Apoptosis* 2007;12:897–911. [PubMed: 17453159]
11. Annis MG, Soucie EL, Dlugosz PJ, Cruz-Aguado JA, Penn LZ, Leber B, Andrews DW. Bax forms multispansing monomers that oligomerize to permeabilize membranes during apoptosis. *EMBO J* 2005;24:2096–2103. [PubMed: 15920484]
12. Mikhailov V, Mikhailova M, Degenhardt K, Venkatachalam MA, White E, Saikumar P. Association of Bax and Bak homo-oligomers in mitochondria: Bax requirement for Bak reorganization and cytochrome c release. *J. Biol. Chem* 2003;278:5367–5376. [PubMed: 12454021]
13. Mikhailov V, Mikhailova M, Pulkrabek DJ, Dong Z, Venkatachalam MA, Saikumar P. Bcl-2 prevents Bax oligomerization in the mitochondrial outer membrane. *J. Biol. Chem* 2001;276:18361–18374. [PubMed: 11279112]
14. Gross A, Jockel J, Wei MC, Korsmeyer SJ. Enforced dimerization of BAX results in its translocation, mitochondrial dysfunction and apoptosis. *EMBO J* 1998;17:3878–3885. [PubMed: 9670005]
15. Uren RT, Dewson G, Chen L, Coyne SC, Huang DCS, Adams JM, Kluck RM. Mitochondrial permeabilization relies on BH3 ligands engaging multiple prosurvival Bcl-2 relatives, not Bak. *J Cell Biol* 2007;177(2):277–287. [PubMed: 17452531]
16. Willis SN, Fletcher JI, Kaufmann T, van Delft MF, Chen L, Czabotar PE, Ierino H, Lee EF, Fairlie WD, Bouillet P, Strasser A, Kluck RM, Adams JM, Huang DCS. Apoptosis initiated when BH3 ligands engage multiple Bcl-2 homologs, not Bax or Bak. *Science* 2007;315:856–859. [PubMed: 17289999]
17. Kim H, Rafiuddin-Shah M, Tu HC, Jeffers JR, Zambetti GP, Hsieh JJ, Cheng EH. Hierarchical regulation of mitochondrion-dependent apoptosis by BCL-2 subfamilies. *Nat Cell Biol* 2006;8:1348–1358. [PubMed: 17115033]
18. Schlesinger PH, Gross A, Xin XM, Yamamoto K, Saito M, Waksman G, Korsmeyer SJ. Comparison of the ion channel characteristics of pro apoptotic bax and anti-apoptotic bcl-2. *Proc. Natl. Acad. Sci. U.S.A* 1997;94:11357–11362. [PubMed: 9326614]
19. Saito M, Korsmeyer SJ, Schlesinger PH. Bax dependent cytochrome-c transport reconstituted in pure liposomes. *Nature Cell Biology* 2000;2:553–555.
20. Westover EJ, Covey DF. The enantiomer of cholesterol. *J. Memb. Biol* 2004;202:61–72.
21. Mouritsen OG, Zuckermann MJ. What's so special about cholesterol? *Lipids* 2004;39:1101–1113. [PubMed: 15726825]
22. Soccio RE, Breslow JL. Intracellular cholesterol transport. *Arterioscler Thromb Vasc Biol* 2004;24:1150–1160. [PubMed: 15130918]
23. Cheng B, Hsu DK, Kimura T. Utilization of intramitochondrial membrane cholesterol by cytochrome P-450-dependent cholesterol side-chain cleavage reaction in bovine adrenocortical mitochondria: steroidogenic and non-steroidogenic pools of cholesterol in the mitochondrial inner membranes. *Mol Cell Endocrinol* 1985;40:233–243. [PubMed: 4007257]
24. Tuckey RC, Headlam MJ, Bose HS, Miller WL. Transfer of cholesterol between phospholipid vesicles mediated by the steroidogenic acute regulatory protein (StAR). *J. Biol. Chem* 2002;277:47123–47128. [PubMed: 12372832]
25. Leonarduzzi G, Biasi F, Chiarpotto Giuseppe Poli E. Trojan horse-like behavior of a biologically representative mixture of oxysterols. *Mol. Aspects Med* 2004;25:155–167. [PubMed: 15051324]
26. Lacapere JJ, Papadopoulos V. Peripheral-type benzodiazepine receptor: structure and function of a cholesterol-binding protein in steroid and bile acid biosynthesis. *Steroids* 2003;68:569–585. [PubMed: 12957662]
27. Casellas P, Galiegue S, Basile AS. Peripheral benzodiazepine receptors and mitochondrial function. *Neurochem. Internat* 2002;40:475486.

28. Jamin N, Neumann J-M, Ostuni MA, Ngoc Vu TK, Yao Z-X, Murail S, Robert J-C, Giatzakis C, Papadopoulos V, Lacapère J-J. Characterization of the cholesterol recognition amino acid consensus sequence of the peripheral-type benzodiazepine receptor. *Molecular Endocrinology* 2005;19:588–594. [PubMed: 15528269]
29. Russell DW. Oxysterol biosynthetic enzymes. *Biochim. Biophys. Acta* 2000;1529:126–135. [PubMed: 11111082]
30. Omura T. Mitochondrial P450s. *Chem Biol Interact* 2006;163:86–93. [PubMed: 16884708]
31. Feo F, Canuto RA, Bertone G, Garcea R, Pani P. Cholesterol and phospholipids composition of mitochondria and microsomes isolated from Morris hepatoma 5123 and rat liver. *FEBS Lett* 1973;33:229–333. [PubMed: 4354064]
32. Campbell AM, Chan SHP. The voltage dependent anion channel affects mitochondrial cholesterol distribution and function. *Arch Biochem Biophys* 2007;466:203–210. [PubMed: 17662230]
33. Lucken-Ardjomande S, Montessuit S, Martinou J-C. Bax activation and stress-induced apoptosis delayed by the accumulation of cholesterol in mitochondrial membranes. *Cell Death and Differentiation* 2007;15:484–493. [PubMed: 18084240]
34. Martinez-Abundis E, Garcia N, Correa F, Franco M, Zazueta C. Changes in specific lipids regulate BAX-induced mitochondrial permeability transition. *FEBS Journal* 2007;274:6500–6510. [PubMed: 18028444]
35. Chen C, Cui J, Lu H, Wang R, Zhang S, Shen P. Modeling of the role of a Bax-activation switch in the mitochondrial apoptosis decision. *Biophys J* 2007;92:4304–4315. [PubMed: 17400705]
36. Er E, Oliver L, Cartron P-F, Juin P, Manon S, Vallette FM. Mitochondria as the target of the pro-apoptotic protein bax. *Biochim. Biophys. Acta* 2006;1757:1301–1311. [PubMed: 16836974]
37. Cartron P-F, Arokium H, Oliver L, Meflah K, Manon S, Vallette FM. Distinct domains control the addressing and the insertion of Bax into mitochondria. *J. Biol. Chem* 2005;280:10587–10598. [PubMed: 15590655]
38. Kroemer G, Galluzzi L, Brenner C. Mitochondrial membrane permeabilization in cell death. *Physiol Rev* 2007;87:99–163. [PubMed: 17237344]
39. Cortese JD, Voglino AL, Hackenbrock CR. Ionic strength of the intermembrane space of intact mitochondria as estimated with fluorescein-BSA delivered by low pH fusion. *J. Cell Biol* 1991;113:1331–1340. [PubMed: 2045415]
40. Gupte SS, Hackenbrock CR. The role of cytochrome c diffusion in mitochondrial electron transport. *J. Biol. Chem* 1988;263:5248–5253. [PubMed: 2833502]
41. Schikorski T, Stevens CF. Morphological correlates of functionally defined synaptic vesicle populations. *Nature Neuroscience* 2001;4:391–395.
42. Deerinck TJ, Martone ME, Lev-Ram V, Green DP, Tsien RY, Spector DL, Huang S, Ellisman MH. Fluorescence photooxidation with eosin: a method for high resolution immunolocalization and in situ hybridization detection for light and electron microscopy. *J. Cell Biol* 1994;126:901–910. [PubMed: 7519623]
43. Komarov AG, Deng D, Craigen WJ, Colombini M. New insights into the mechanism of permeation through large channels. *Biophys. J* 2005;89:3950–3959. [PubMed: 16199505]
44. Hulbert AJ, Turner N, Hinde J, Else P, Guderley H. How might you compare mitochondria from different tissues and different species? *J Comp Physiol B* 2006;176:93–105. [PubMed: 16408229]
45. Bathori G, Csordas G, Garcia-Perez C, Davies E, Hajnoczky G. Ca²⁺-dependent control of the permeability properties of the mitochondrial outer membrane and voltage-dependent anion-selective channel (VDAC). *J Biol Chem* 2006;281:17347–17358. [PubMed: 16597621]
46. Pavlov E, Grigoriev SM, Dejean LM, Zweihorn CL, Mannella CA, Kinnally KW. The mitochondrial channel VDAC has a cation-selective open state. *Biochim. Biophys. Acta* 2005;1716:96–102. [PubMed: 16293222]
47. Rostovtseva T, Colombini M. VDAC channels mediate and gate the flow of ATP: implications for the regulation of mitochondrial function. *Biophysical J* 1997;72:1954–1962.
48. Rostovtseva TK, Tan W, Colombini M. On the role of VDAC in apoptosis: Fact and fiction. *J. Bioenerget. Biomemb* 2005;37:129–142.

49. Schein SJ, Colombini M, Finkelstein A. Reconstitution in planar lipid bilayers of a voltage-dependent anion-selective channel obtained from paramecium mitochondria. *J. Membrane Biol* 1976;30:99–120. [PubMed: 1011248]
50. Scorrano L, Oakes SA, Opferman JT, Cheng EH, Sorcinelli MD, Pozzan T, Korsmeyer SJ. Bax and bak regulation of endoplasmic reticulum Ca^{2+} : A control point for apoptosis. *Science* 2003;300:135–139. [PubMed: 12624178]
51. Feigenson GW. Phase boundaries and biological membranes. *Annu. Rev. Biophys. Biomol. Struct* 2007;36:63–77. [PubMed: 17201675]
52. Hung WC, Lee MT, Chen FY, Huang HW. The condensing effect of cholesterol in lipid bilayers. *Biophys. J* 2007;92:3960–3967. [PubMed: 17369407]
53. Smaby JM, Momsen MM, Brockman HL, Brown RE. Phosphatidylcholine acyl unsaturation modulates the decrease in interfacial elasticity induced by cholesterol. *Biophys. J* 1997;73:1492–1505. [PubMed: 9284316]
54. Goping IS, Gross A, Lavoie JN, Nguyen M, Jemmerson R, Roth K, Korsmeyer SJ, Shore GC. Regulated targeting of BAX to mitochondria. *J. Cell Biol* 1998;143:207–215. [PubMed: 9763432]
55. Wolter KG, Hsu Y-T, Smith CL, Nechushtan A, Xi X-G, Youle RJ. Movement of bax from the cytosol to mitochondria during apoptosis. *J. Cell Biol* 1997;139:1281–1292. [PubMed: 9382873]
56. Cho W, Stahelin RV. Membrane-protein interactions in cell signaling and membrane trafficking. *Annu Rev Biophys Biomol Struct* 2005;34:119–151. [PubMed: 15869386]
57. Erb E-M, Chen X, Allen S, Roberts CJ, Tendler SJB, Davies MC, Forsén S. Characterization of the surfaces generated by liposome binding to the modified dextran matrix of a surface plasmon resonance sensor chip. *Anal. Biochem* 2000;280:29–35. [PubMed: 10805517]
58. Shaposhnikova VV, Egorova MV, Kudryavtsev AA, Kh M, Levitman MKh, Korystov YN. The effect of melittin on proliferation and death of thymocytes. *FEBS Letters* 1997;410:285–288. [PubMed: 9237646]
59. Ownby CL, Powell JR, Jiang MS, Fletcher JE. Melittin and phospholipase A2 from bee (*Apis mellifera*) venom cause necrosis of murine skeletal muscle in vivo. *Toxicol* 1997;35:67–80. [PubMed: 9028010]
60. Youle RJ, Strasser A. The BCL-2 protein family: opposing activities that mediate cell death. *Nature Reviews Molecular Cell Biology* 2008;9:47–59.
61. Harata N, Ryan TA, Smith SJ, Buchanan J, Tsien RW. Visualizing recycling synaptic vesicles in hippocampal neurons by FM 1-43 photoconversion. *Proc. Natl. Acad. Sci. U.S.A* 2001;98:12748–12753. [PubMed: 11675506]
62. Rostovtseva TK, Kazemi N, Weinrich M, Bezrukov SM. Voltage gating of vDAC is regulated by nonlamellar lipids of mitochondrial membranes. *J Biol Chem* 2006;281:37496–37506. [PubMed: 16990283]
63. Cortese JD, Hackenbrock CR. Motional dynamics of functional cytochrome c delivered by low pH fusion into the intermembrane space of intact mitochondria. *Biochim. Biophys. Acta* 1993;1142:194–202. [PubMed: 8384490]
64. Willis SN, Adams JM. Life in the balance: how BH3-only proteins induce apoptosis. *Curr Opin Cell Biol* 2005;17:617–625. [PubMed: 16243507]
65. Cheng EH-Y, Sheiko TV, Fisher JK, Craigen WJ, Korsmeyer CV. VDAC2 inhibits BAK activation and mitochondrial apoptosis. *Science* 2003;301:513–517. [PubMed: 12881569]
66. Rouslin W, MacGee J, Gupte S, Wesselman A, Epps DE. Mitochondrial cholesterol content and membrane properties in porcine myocardial ischemia. *Am. J. Physiol* 1982;242:H254–H259. [PubMed: 6461257]
67. Hauser, H.; Poupart, G. *The Structure of Biological Membranes*. 2 edition. CRC Press; 2005. p. 1-53.
68. Epand RM. Cholesterol and the interaction of proteins with membrane domains. *Prog. Lip. Res* 2006;45:279–294.
69. Crowder CM, Westover EJ, Kumar AS Jr, Ostlund RE, Covey DF. Enantiospecificity of cholesterol function in vivo. *J. Biol. Chem* 2001;276:44369–44372. [PubMed: 11598105]
70. Alakoskela, Juha-Matti; Sabatini, Karen; Jiang, Xin; Laitala, Venla; Covey, Douglas F.; Kinnunen, Paavo KJ. On enantiospecific interactions between cholesterol and phospholipids. *Langmuir* 2008;24:830–836. [PubMed: 18171092]

71. Grain RC, Clark RW, Harvey BE. Role of lipid transfer proteins in the abnormal lipid content of morris hepatoma mitochondria and microsomes. *Cancer Research* 1983;43:3197–3202. [PubMed: 6850630]
72. Graham JM, Green C. The properties of mitochondria enriched in vitro with cholesterol. *Eur. J. Biochem* 1970;12:58–66. [PubMed: 4313981]
73. Werner M, Sacher J, Hohenegger M. Mutual amplification of apoptosis by statin-induced mitochondrial stress and doxorubicin toxicity in human rhabdomyosarcoma cells. *Br J Pharmacol* 2004;143:715–724. [PubMed: 15289292]
74. Anderluh, Gregor; Mačeka, P.; Lakey, JH. Peeking into a secret world of pore-forming toxins: membrane binding processes studied by surface plasmon resonance. *Toxicon* 2003;42:225–228. [PubMed: 14559072]
75. Bavdek A, Gekara NO, Priselac D, Aguirre IG, Darji A, Chakraborty T, Macek P, Lakey JH, Weiss S, Anderluh G. Sterol and pH interdependence in the binding, oligomerization, and pore formation of listeriolysin o. *Biochemistry* 2007;46:4425–4437. [PubMed: 17358050]
76. Bastos M, Bai G, Gomes P, Andreu D, Goormaghtigh E, Prieto M. Energetics and partition of two cecropinmelittin hybrid peptides to model membranes of different composition. *Biophys J* 2007;94:2128–2141. [PubMed: 18032555]
77. Besenicar M, Macek P, Lakey JH, Anderluh G. Surface plasmon resonance in protein-membrane interactions. *Chem Phys Lipids* 2006;141:169–178. [PubMed: 16584720]
78. Papo N, Shai Y. Exploring peptide membrane interaction using surface plasmon resonance: differentiation between pore formation versus membrane disruption by lytic peptides. *Biochemistry* 2003;42:458–466. [PubMed: 12525173]
79. Ali S, Smaby JM, Brockman HL, Brown RE. Cholesterol's interfacial interactions with galactosylceramides. *Biochemistry* 1994;33:2900–2906. [PubMed: 8130203]
80. McConnell HM, Vrljic M. Liquid-liquid immiscibility in membranes. *Annu. Rev. Biophys. Biomol. Struct* 2003;32:469–492. [PubMed: 12574063]
81. Szoka F, Papahadjopoulos D. Procedure for preparation of liposomes with large internal aqueous space and high capture by reverse-phase evaporation. *Proc. Nat. Acad. Sci. USA* 1978;75:4194–4198. [PubMed: 279908]
82. Stewart JCM. Colorimetric determination of phospholipids with Ammonium Ferrothiocyanate. *Anal. Biochem* 1980;104:10–14. [PubMed: 6892980]
83. Schlesinger PH, Saito M. The bax pore in liposomes, biophysics. *Cell Death and Differentiation* 2006;13:1403–1408. [PubMed: 16763615]
84. Gokel GW, Schlesinger PH, Djedović NK, Ferdani R, Harder EC, Hu J, Leevy WM, Pajewska J, Pajewska R, Weber ME. Functional, synthetic organic chemical models of cellular ion channels. *Bioorganic & Medicinal Chemistry* 2004;12:1291–1304. [PubMed: 15018901]
85. Djedovic N, Ferdani R, Harder E, Pajewska J, Pajewski R, Weber ME, Schlesinger PH, Gokel GW. The C- and N-terminal residues of synthetic heptapeptide ion channels influence transport efficacy through phospholipid bilayers. *New J. Chem* 2005;29:291–305.
86. Miller C. Ion channels in liposomes. *Ann. Rev. Physiol* 1984;46:549–558. [PubMed: 6324663]
87. Hille, B. *Ionic Channels of Excitable Membranes*. 3 edition. Sunderland, MA: Sinauer Associates Inc.; 2001. chapter 11; p. 347-376.
88. Rex S, Schwarz G. Quantitative studies on the melittin-induced leakage mechanism of lipid vesicles. *Biochemistry* 1998;37:2336–2345. [PubMed: 9485380]
89. Pallotti, F.; Lenaz, G. Mitochondria and mitoplasts from cultured cells. In: Pon, LA.; Schon, EA., editors. *Methods in Cell Biology*. volume 65. Academic Press; 2001. p. 4-31.
90. Frezza, Christian; Cipolat, Sara; Scorrano, Luca. Organelle isolation: functional mitochondria from mouse liver, muscle and cultured fibroblasts. *Nature Protocols* 2007;2:287–295.
91. Mancuso, David J.; Sims, Harold F.; Han, Xianlin; Jenkins, Christopher M.; Guan, Shao Ping; Yang, Kui; Moon, Sung Ho; Pietka, Terri; Abumrad, Nada A.; Schlesinger, Paul H.; Gross, Richard W. Genetic ablation of calcium-independent phospholipase A2gamma leads to alterations in mitochondrial lipid metabolism and function resulting in a deficient mitochondrial bioenergetic phenotype. *J. Biol. Chem* 2007;282:34611–34622. [PubMed: 17923475]

92. Frolov A, Zielinski SE, Crowley JR, Dudley-Rucker N, Schaffer JE, Ory DS. NPC1 and NPC2 regulate cellular cholesterol homeostasis through generation of low density lipoprotein cholesterol-derived oxysterols. *J. Biol. Chem* 2003;278:25517–25525. [PubMed: 12719428]
93. Nicholls, DG.; Ferguson, SJ. *Bioenergetics*. 3. London: Academic Press; 2001. chapter 5:Respiratory Chains; p. 89-154.
94. Anderluh G, Besenicar M, Kladnik A, Lakey JH, Macek P. Properties of nonfused liposomes immobilized on an L1 biacore chip and their permeabilization by a eukaryotic pore-forming toxin. *Anal. Biochem* 2005;344:43–52. [PubMed: 16039981]
95. Fleming KG. Standardizing the free energy change of transmembrane helix-helix interactions. *J. Mol. Biol* 2002;323:563–571. [PubMed: 12381309]

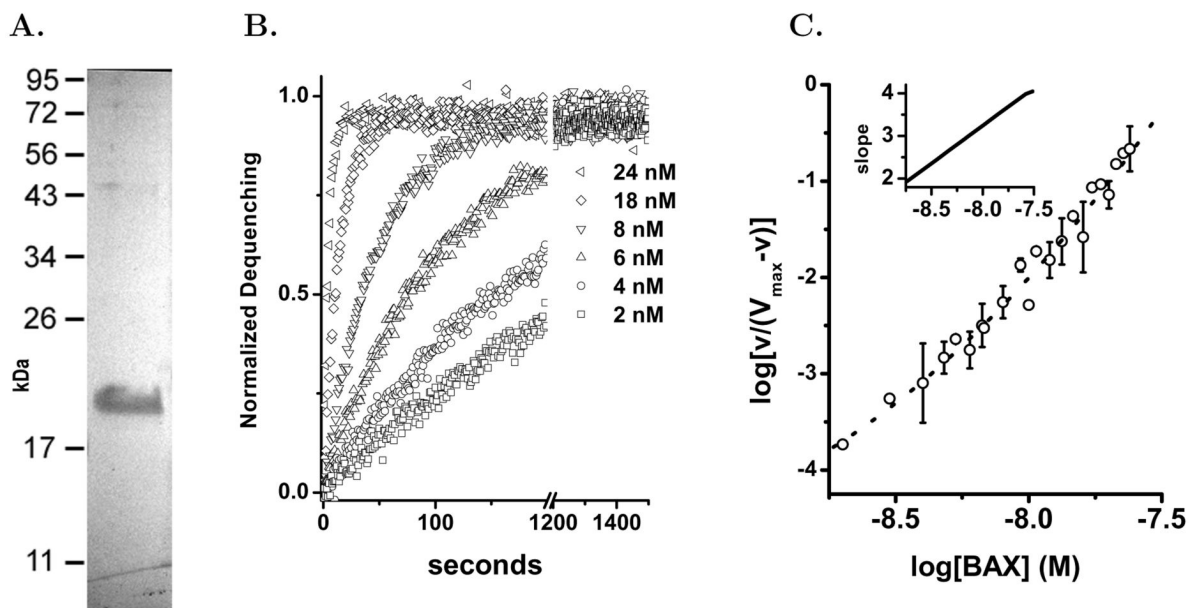


Figure 1. Human $\text{BAX}(\Delta\text{C19})$ Pore Forming Activity in Liposomes

Using human $\text{BAX}(\Delta\text{C19})$ we studied the kinetics of pore activation in liposomes by the purified protein. The liposome assay was done as previously described[19]. **Panel A.** Preparation of human $\text{BAX}(\Delta\text{C19})$ expressed and purified as described in Methods and run on SDS-PAGE gel to demonstrate size and purity. **Panel B** Time series examples of human $\text{BAX}(\Delta\text{C19})$ pore activation as added protein concentration is increased. $\text{BAX}(\Delta\text{C19})$ concentrations shown are: \triangleleft –24.8 nM, \circ –16 nM, \triangle –8 nM, ∇ –4.8 nM, \diamond –4 nM, \square –2 nM. Using the time series data curve fitting to an exponential function determined the time constant and the extent of release. **Panel C.** The time constants determined from the time series and concentration dependence of pore activation were subjected to Hill analysis. Each plotted point represents the average of 2–3 determinations with standard deviations shown when they were bigger than the symbol. The data was fitted to a polynomial using the Levenberg-Marquardt algorithm. The slope of the fitted line was determined at each point and is plotted in the inset graph.

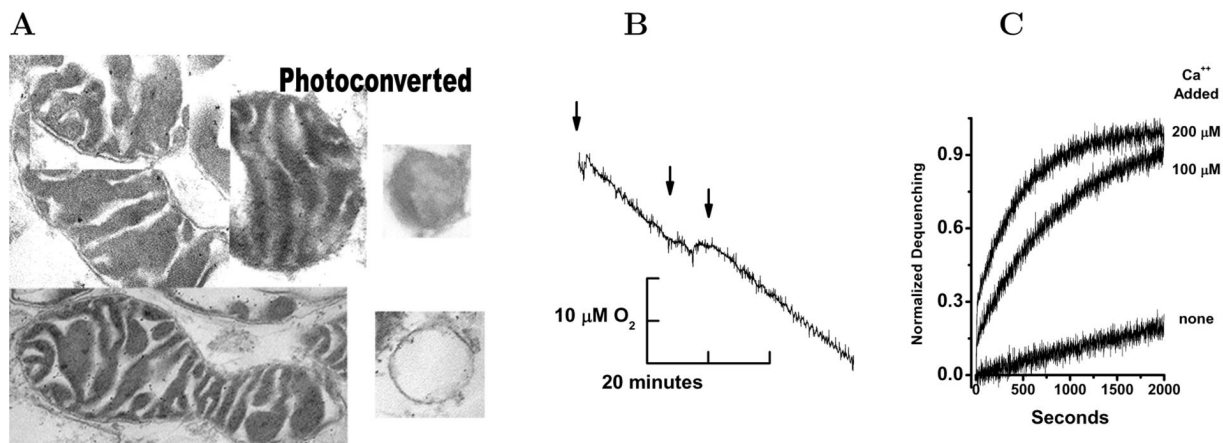


Figure 2. Studies on Isolated Mitochondria After Fusion with CF-Liposomes

Panel A. Mitochondria were prepared and fused with 200 nm liposomes containing 20 mM carboxyfluorescein as described in Methods. These mitochondria were then pelleted, fixed, embedded for sectioning and electron microscopy. In all cases the mitochondria have a traditional two-membrane morphology after fusion with liposomes. Exposure of the isolated mitochondria to UV light photo-converted the CF and photo-oxidized diaminobenzidine producing the electron dense depositions in the intermembrane space. At the right of this panel are two large unilamellar liposomes that were used in the fusion loading of the mitochondria. The upper liposome was photo-converted and the lower was not exposed to UV light, see Methods. **Panel B.** After isolation and fusion with liposomes containing CF the mitochondrial suspension was diluted to 1 mg/ml protein and O_2 consumption was measured. At the first arrow 10 mM ascorbate and TMPD were added initiating rapid O_2 uptake that was dependent upon cytochrome c and cytochrome oxidase, at the second arrow 200 nM melittin was added and at the third arrow 100 μ M horse cytochrome c was added. **Panel C.** Mitochondria were isolated and fused with liposomes as described in Methods in the presence of 1 mM EGTA. Subsequently the washed mitochondrial suspension was diluted 1:100 into the assay buffer or buffer with added 100 μ M or 200 μ M $CaCl_2$ (from bottom to top) and fluorescence dequenching followed for the indicated times. All dequenching values were normalized to the 1% Triton X-100 initiated dequenching.

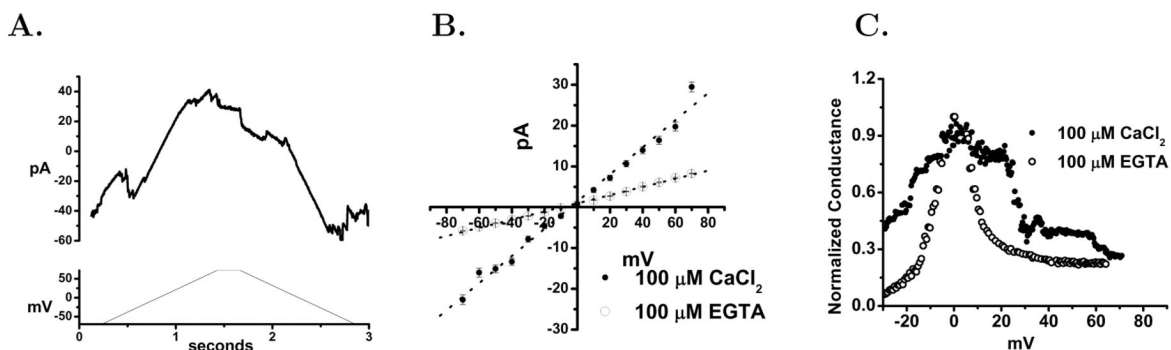


Figure 3. Channel Activity in Membranes of Liposome-Fused Mitochondria

Panel A. Isolated, liposome-fused mitochondria from cultured HeLa cells were studied in planar lipid bilayers as described in Methods. Mitochondria were added to the cis chamber of a planar lipid bilayer cuvette with a 450 to 150 mM KCl from the cis to trans chambers. After 3–7 minutes current levels stabilized and the cis solution was perfused to 150 mM KCl. Using voltage clamp configuration command ramps (lower panel) were applied to the bilayer after fusion events were observed. **Panel B.** Using buffer containing 100 μM CaCl₂ and 100 μM EGTA the stable voltage dependence of fM was studied. Data were obtained by holding indicated the membrane potential for 10 seconds and using the the average current of the final two seconds. EGTA to 100 μM was added to the cis chamber and after 5 minutes the voltage dependence was determined again. The high calcium perfusion, voltage dependence, EGTA addition and voltage dependence re-determination was repeated until the bilayer membrane collapsed, 3 cycles. These were averaged for this panel and the s.d. at each point shown in the figure. **Panel C.** Bilayer conductance was calculated from voltage ramps (± 60 mV) collected at 1.67 kHz with a 1.2 second duration for each ramp. The bilayers were formed and Ca²⁺ concentration adjusted as described in Panel A. The currents were normalized to a peak conductance of 1 for comparison.

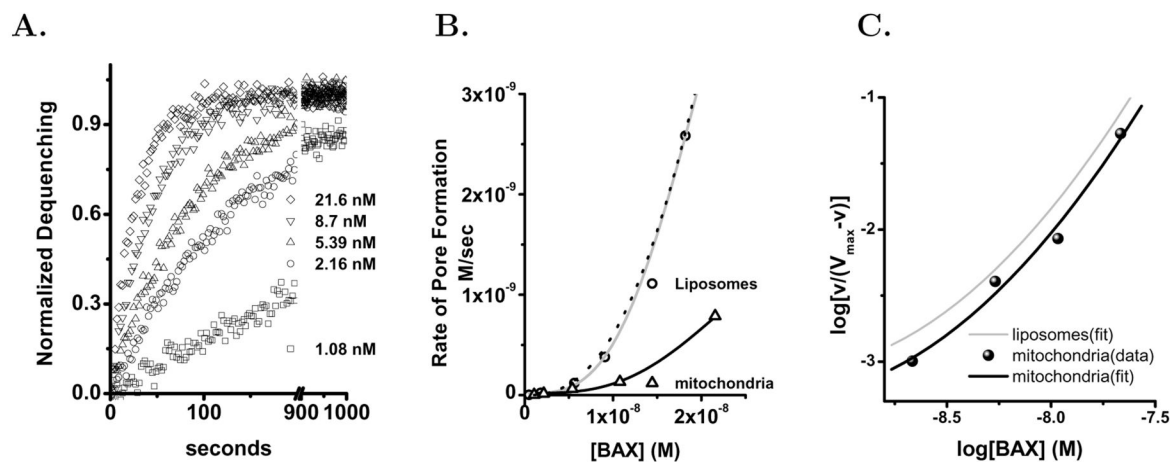


Figure 4. Bax Pore Activation in Isolated Mitochondria

Mitochondria were isolated from cultured HeLa cells and fused with liposomes using a modification of a previously described technique as described in the Methods. **Panel A.** Mitochondria were diluted into a 500 μ L assay volume to give a protein concentration of 0.3 mg/ml and a phospholipid concentration of 4.3 μ M. The concentrations of BAX(Δ C19) are as follows: \square -1 nM, \circ -2.2 nM, Δ -5.4 nM, ∇ -8.7 nM and \diamond -21.6 nM. The fractional dequenching was fitted to an exponential model in order to determine the time constant (τ) for analysis of the kinetics of BAX pore activation. **Panel B.** Comparison of the rate of BAX(Δ C19) pore activation in mitochondria Δ and liposomes \circ . Both sets of data are fitted by Hill functions (black and gray lines respectively). The rate of pore activation in mitochondria was then normalized for the increased lipid in this assay and then was fitted by the dotted black line. The normalized pore activation data points are not shown in this panel. **Panel C.** The pore activation time constants that have been normalized for lipid concentration are plotted in the standard logarithmic form for Hill analysis. The data was fitted as in Figure 1 and the fitted curve plotted in black. The liposome fitted line is shown in gray for comparison.

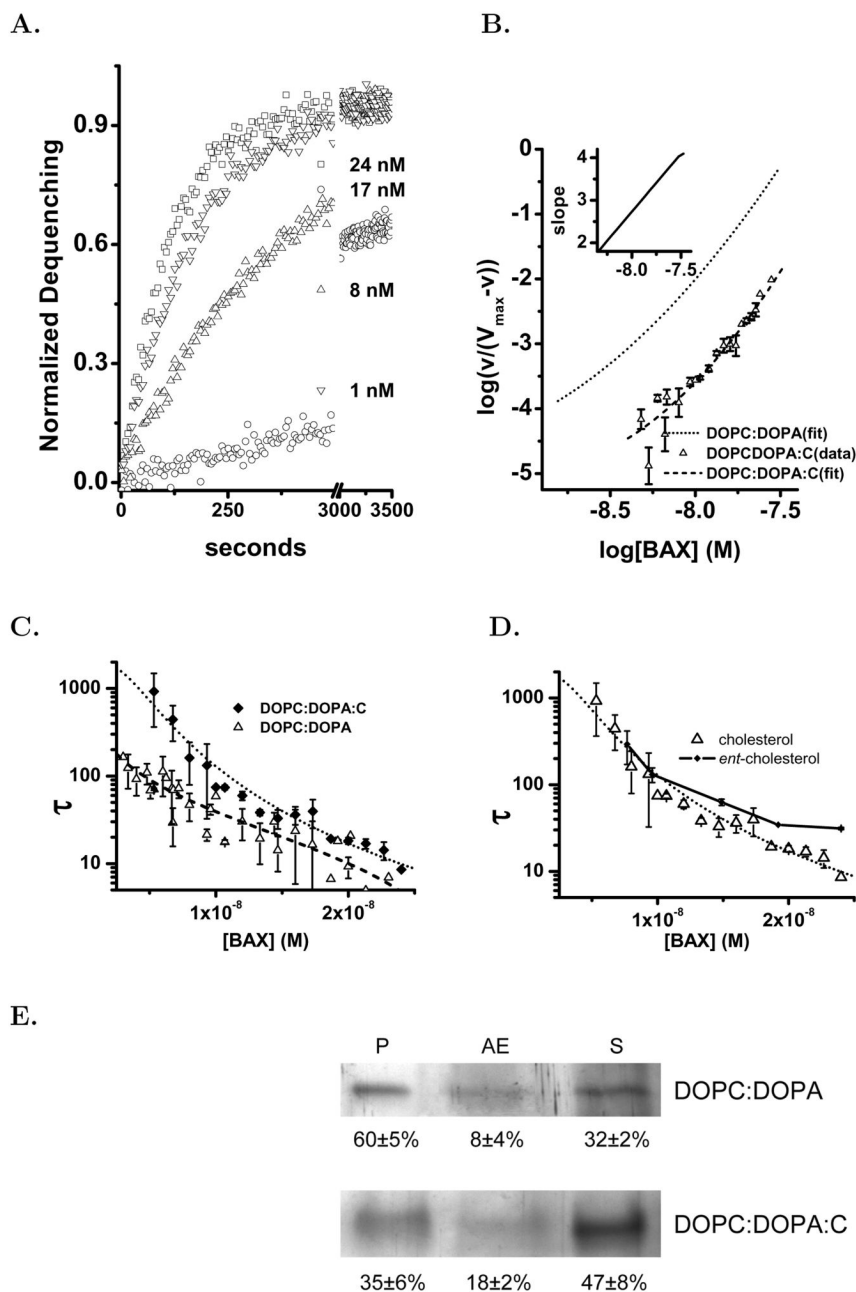


Figure 5. BAX Pore Activation and Binding in DOPC:DOPA:C Liposomes

Liposomes containing cholesterol were prepared as described in Methods. **Panel A.** Selected examples of time series dequenching by human $BAX(\Delta C19)$ in DOPC:DOPA:C (mole fraction 0.59:0.21:0.20) liposomes. Human $BAX(\Delta C19)$ concentrations were: \circ -1, Δ -8, ∇ -17, and \square -24 nM. Fractional dequenching was computed by comparison with Triton X-100 dequenching.

Panel B. Hill analysis of the human $BAX(\Delta C19)$ pore activation in DOPC:DOPA:C liposomes. Each determination of the time constant is shown with the s.d. error bars ($n \geq 3$). The series of time constants was fitted to a polynomial and the slope of the fitted line determined and presented in the inset plot. Also shown is the fitting from Figure 1C in DOPC:DOPA liposomes

as a the dotted line. **Panel C.** Comparison of the concentration dependence of the time constant for pore activation in DOPC:DOPA (Δ) and DOPC:DOPA:C (\blacklozenge) liposomes. Each of the determinations is shown with s.d. ($n \geq 3$). Dotted lines are the nonlinear least squares fitting of the time constants to the Hill equation. **Panel D.** Comparison of B_{AX} pore activation in liposomes composed of DOPC:DOPA:C (Δ) and DOPC:DOPA:*entC* (mole fraction 0.59:0.21:0.20) (\circ). Each of the determinations is shown with s.d. ($n \geq 3$). Dotted lines are the nonlinear least squares fitting of the time constants to the Hill equation. **Panel E.** Defined liposomes were suspended in 200 nM $B_{AX}(\Delta C19)$ and incubated for 10 minutes at room temperature. As indicated in the figure the liposomes were \pm cholesterol. The liposomes were sedimented at 150,000 \times g as described in Methods to give the pellet (P) and alkaline extraction (AE) or supernatant (S). Each sample was separated by SDS-PAGE with silver staining. The region at 19–20 kD of the gel was analyzed for density and the percent distribution of the protein in each fraction was calculated for the figure.

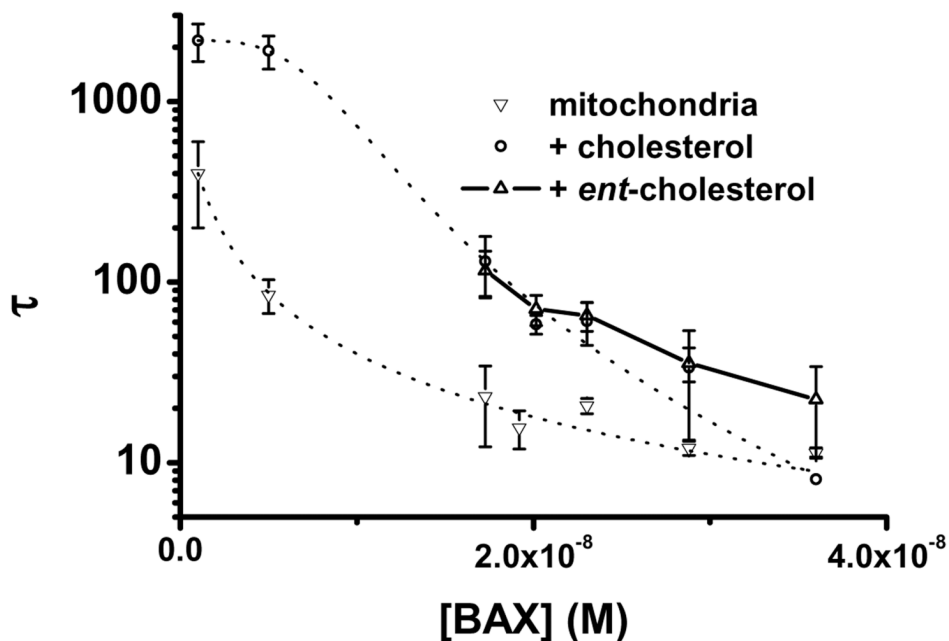


Figure 6. Effect of Sterol on $BAX(\Delta C19)$ Pore Activation in Mitochondria

The effect of cholesterol on BAX pore activation in isolated mitochondria fused with liposomes containing 20 mol% cholesterol. Pore activation in these mitochondria, \circ , was greatly reduced compared to mitochondria fused with DOPC:DOPA liposomes, ∇ . Mitochondria were also fused with liposomes prepared using the enantiomer of cholesterol, Δ . The dotted lines are the results of nonlinear least squares fitting the time constants for pore activation in mitochondria fused to liposomes and cholesterol-liposomes. Time constants of pore activation in mitochondria fused with liposomes prepared with the enantiomer of cholesterol are not fitted.

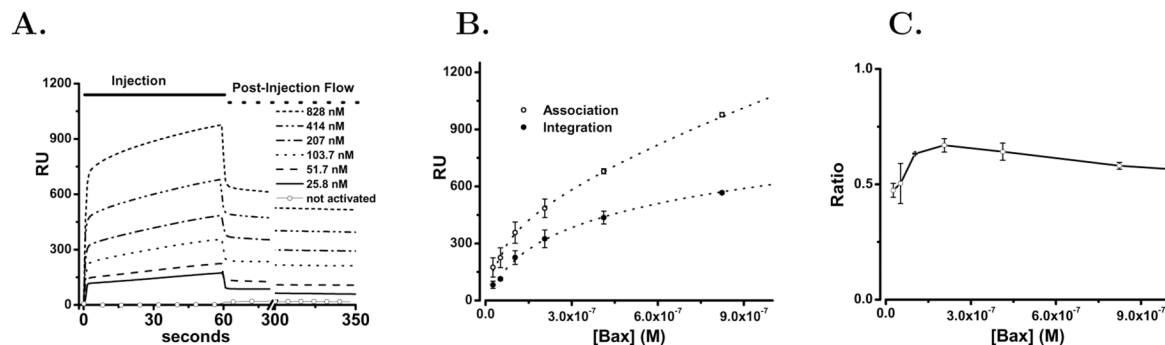


Figure 7. BAX Binding to Supported DOPC/DOPA Liposomes

The binding and membrane integration of BAX(Δ C19) was studied by surface plasmon resonance using supported liposomes. **Panel A.** BAX(Δ C19) was injected over an L1 chip covered with immobilized DOPC/DOPA (74:26 mol%) liposomes as described in Methods. This protein was prepared as described above without using detergent. Prior to exposure of the BAX(Δ C19) to detergent the protein did not bind to the liposomes as shown by the open circles ($\circ \circ \circ$) at the bottom of the graph that indicate the averaged RU response for the 25–3000 nM BAX(Δ C19) concentration range. After treatment with detergent the RU response for the following concentrations is shown: 25.8 nM (solid), 51.8 nM (dash), 103.5 nM (Dot), 207 nM (Dash-dot), 414 nM (dash-dot-dot), 828 nM (short dash). The injection phase is indicated by the solid line and the wash phase by the dashed line at the top of the graph. **Panel B.** Comparison of membrane-associated (\square) and membrane-integrated (\circ) protein using the criteria described in the text and calculating the average values and S.D. as described in Methods. The dotted lines represent the best fit to a interaction model as described in the text. **Panel C.** The ratio of binding and integration fraction of protein plotted as the added concentration of BAX(Δ C19) is increased. Means and standard deviations are computed as described in the methods.

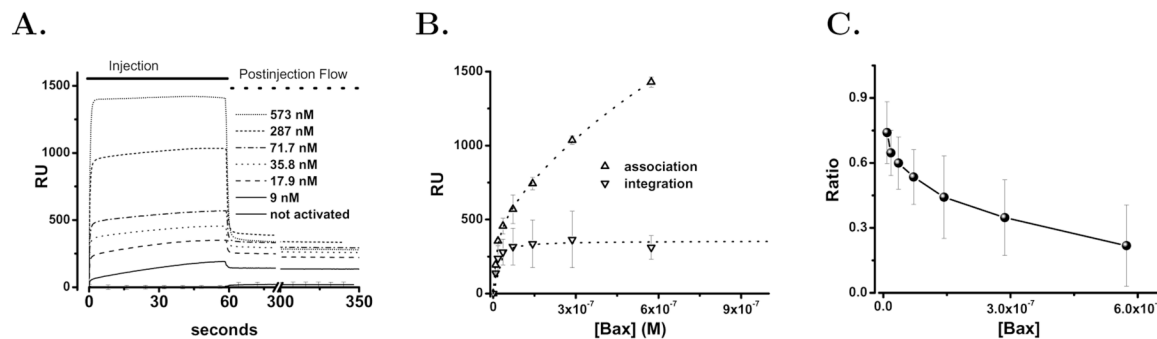


Figure 8. BAX Binding To Supported DOPC/DOPA/Cholesterol Containing Liposomes

The binding and membrane integration of BAX(Δ C19) was studied by surface plasmon resonance using supported liposomes containing cholesterol. **Panel A.** BAX(Δ C19) was injected over an L1 chip covered with DOPC:DOPA:C (59:21:20 mol%) liposomes. This protein was prepared as described in Methods without using detergent. Prior to exposure of the BAX(Δ C19) to detergent the protein did not bind to the liposomes as shown by the open circles ($\circ \circ \circ$) at the bottom of the graph that indicate the averaged RU response for the 25–3000 nM BAX(Δ C19) concentration range of unactivated protein. After treatment with detergent the RU response for the following concentrations is shown: 9 nM (solid), 18 nM (dash), 36 nM (Dot), 72 nM (Dash-dot), 289 nM (dash-dot-dot), 574 nM (short dash). The injection phase is indicated by the solid line and the wash phase by the dashed line at the top of the graph. **Panel B.** Comparison of membrane-associated (Δ) and membrane-integrated (∇) protein using the criteria described in the text and calculating the average values and S.D. as described in Methods. The dotted lines represent the best fit to an interaction model as described in the text. **Panel C.** The ratio of binding and integration of protein plotted as the fraction integrated as concentration of BAX(Δ C19) is increased. Means and standard deviations are computed as described in the Methods.

Table 1Analysis of ^{BAX} Membrane Interaction

Kind of Membrane Interaction ²	K_1 M	^{BAX} Mole Fraction ³ DOPC:DOPA	K_2 M	^{BAX} Mole Fraction ³
Membrane Binding	$2.2 \pm 0.4 \times 10^{-6}$	$5.9 \pm 0.7 \times 10^{-3}$	$1.37 \pm 0.45 \times 10^{-8}$	$0.78 \pm 0.31 \times 10^{-3}$
Membrane Integration			$2.5 \pm 0.27 \times 10^{-7}$	$1.8 \pm 0.07 \times 10^{-3}$
Membrane Binding	$1.6 \pm 1.2 \times 10^{-6}$	$8.6 \pm 4.2 \times 10^{-3}$	$1.4 \pm 0.46 \times 10^{-8}$	$1.2 \pm 0.2 \times 10^{-3}$
Membrane Integration			$1.06 \pm 0.22 \times 10^{-8}$	$0.86 \pm 0.3 \times 10^{-3}$

² As described in the text the ^{BAX} membrane populations were identified by binding and integration with the membrane.

³ We have used mole fraction to represent membrane associated ^{BAX} populations to allow a direct comparison between experiments as a membrane concentration [94].